

MIT Open Access Articles

Quantum Mutual Information Capacity for High-Dimensional Entangled States

The MIT Faculty has made this article openly available. **Please share** how this access benefits you. Your story matters.

Citation: Dixon, P. et al. "Quantum Mutual Information Capacity for High-Dimensional Entangled States." *Physical Review Letters* 108.14 (2012). © 2012 American Physical Society

Published Version: <http://dx.doi.org/10.1103/PhysRevLett.108.143603>

Publisher: American Physical Society

Permanent Link: <http://hdl.handle.net/1721.1/71626>

Version: Final published version: final published article, as it appeared in a journal, conference proceedings, or other formally published context

Terms of use: Article is made available in accordance with the publisher's policy and may be subject to US copyright law. Please refer to the publisher's site for terms of use.



Quantum Mutual Information Capacity for High-Dimensional Entangled States

P. Ben Dixon,* Gregory A. Howland, James Schneeloch, and John C. Howell

Department of Physics and Astronomy, University of Rochester, Rochester, New York 14627, USA
(Received 5 August 2011; revised manuscript received 2 February 2012; published 5 April 2012)

High-dimensional Hilbert spaces used for quantum communication channels offer the possibility of large data transmission capabilities. We propose a method of characterizing the channel capacity of an entangled photonic state in high-dimensional position and momentum bases. We use this method to measure the channel capacity of a parametric down-conversion state by measuring in up to 576 dimensions per detector. We achieve a channel capacity over 7 bits/photon in either the position or momentum basis. Furthermore, we provide a correspondingly high-dimensional separability bound that suggests that the channel performance cannot be replicated classically.

DOI: [10.1103/PhysRevLett.108.143603](https://doi.org/10.1103/PhysRevLett.108.143603)

PACS numbers: 42.50.Dv, 03.67.Bg, 03.67.Hk

Typical examples of quantum entanglement involve two-dimensional bipartite systems [1,2]; however, quantum systems can exhibit more complex forms of entanglement, and attention has recently been turned to studying these rich forms of entanglement. This includes research on entanglement in multiple degrees of freedom (known as “hyperentanglement”) [3,4], as well as high-dimensional systems entangled in a single degree of freedom. These degrees of freedom include time and energy, and transverse-position and momentum (including angular momentum) [5–10]. Both of these types of entanglement can present advantages for practical applications. Indeed, for communication purposes—such as quantum key distribution [11] or dense coding [12]—higher dimensional states increase quantum channel capacity and offer additional benefits such as increased security [13,14].

The photonic transverse-position degree of freedom is a good candidate for practical high-dimensional entangled systems due to the wide availability of technology for manipulating this degree of freedom. As a result there has been significant theoretical and experimental effort to increase and characterize the channel capacity of entangled photons in this transverse domain. Pors *et al.* demonstrated a measurement-limited Shannon dimensionality (the effective number of measurable modes, see [15]) of $D \approx 6$ using angular phase plates for a system with a Schmidt number of $K \approx 31$ [16]. Dada *et al.* demonstrated a violation of an 11-dimensional Bell inequality using spatial light modulators as mode sorters for orbital angular momentum states [17].

These examples show how previous characterization schemes rely on reconstructing continuous transformation properties of the state, which are in general determined either by direct measurement or by reconstructing the density matrix. The reconstruction is then used to calculate the corresponding channel capacity. These methods, however, are difficult to scale to arbitrary dimensions; either the analyzer fabrication requirements exceed the state of the art (e.g., Pors *et al.* anticipated a future Shannon

dimensionality realization of $D \approx 50$), the crosstalk between mode decompositions becomes too large, or the calculations involve very demanding maximization procedures.

Here we propose a direct way of characterizing the communication capabilities of a high-dimensional quantum system—entangled in the photonic transverse-position degree of freedom—that offers several advantages over other methods. This method does not have the intermediate step of determining the transformation properties of the state, but rather uses the knowledge of mutually unbiased bases for our quantum system (the position basis and the momentum basis). This allows us to characterize the system by only measuring in these two bases, drastically reducing the number of required measurements and, in the process, bypassing many of the scaling problems of previous methods. Additionally, this method has the practical benefit of using the communication apparatus itself for the characterization, thus simplifying system requirements and more directly linking the characterization to the system’s ultimate communication capabilities.

We demonstrate the utility of this method on a parametric down-conversion state with a Schmidt number in excess of 1000. Employing classical definitions of mutual information for joint photon detections, and measuring in up to 576 dimensions per detector, we show that the system achieved a channel capacity of over 7 bits per joint photon detection event, roughly equivalent to a dimensionality of 128. We show that this high-dimensional entangled system relies upon quantum correlations by violating the correspondingly high-dimensional classical separability bound. We also show that for Gaussian correlated states in the low-noise limit and as the number of detectors becomes large, the mutual information characterization asymptotically approaches the Schmidt number of the entangled bipartite state.

We characterize our channel using the concept of mutual information, which describes how much information can be determined about a random variable A , by knowing the

value of a correlated random variable B [18,19]. Variables A and B are characterized by the values they take a and b , respectively, and the probability of these values $p(a)$ and $p(b)$, respectively. The mutual information can be written as

$$I(A; B) = H(A) + H(B) - H(A, B), \quad (1)$$

where, for example,

$$H(A) = - \sum_{a \in A} p(a) \log p(a) \quad (2)$$

is the marginal entropy of A , and

$$H(A, B) = - \sum_{\substack{a \in A \\ b \in B}} p(a, b) \log p(a, b) \quad (3)$$

is the joint entropy of A and B . The function $p(a, b)$ is the joint probability distribution that characterizes the correlation between A and B .

We created a position-momentum entangled state using spontaneous parametric down-conversion (SPDC). The state, represented both in position and in momentum, is approximated as [20]

$$\begin{aligned} |\psi\rangle &= \int d\vec{x}_a d\vec{x}_b f(\vec{x}_a, \vec{x}_b) \hat{a}_a^\dagger \hat{a}_b^\dagger |0\rangle \\ &= \int d\vec{k}_a d\vec{k}_b \tilde{f}(\vec{k}_a, \vec{k}_b) \hat{a}_a^\dagger \hat{a}_b^\dagger |0\rangle, \end{aligned} \quad (4)$$

where \hat{a}^\dagger is the photon creation operator. Subscript a indicates the photon is created in the signal mode and subscript b indicates the photon is created in the idler mode, which are then sent to Alice or Bob, respectively. The function

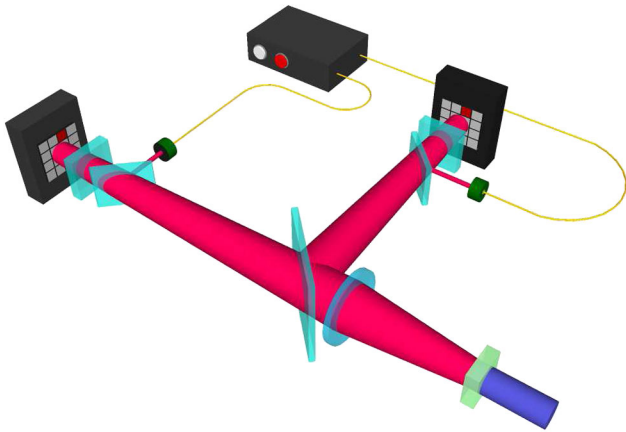


FIG. 1 (color online). Experimental setup. A collimated laser beam undergoes spontaneous parametric down-conversion at a nonlinear crystal. The output passes a focusing lens followed by a beam splitter. The outputs from the beam splitter are sent to digital micromirror devices at either image planes or Fourier planes of the crystal. The micromirror devices are set to retro-reflect the beams, a quarter wave plate and a polarizing beam splitter send the retroreflected beam to a single-photon detector. A coincidence circuit correlates these measurements.

$$f(\vec{x}_a, \vec{x}_b) = N \exp\left(\frac{-(\vec{x}_a - \vec{x}_b)^2}{4\sigma_c^2}\right) \exp\left(\frac{-(\vec{x}_a + \vec{x}_b)^2}{16\sigma_p^2}\right) \quad (5)$$

is the approximated entangled biphoton wave function in the position basis, and

$$\begin{aligned} \tilde{f}(\vec{k}_a, \vec{k}_b) &= (4\sigma_p\sigma_c)^2 N \exp(-\sigma_c^2(\vec{k}_a - \vec{k}_b)^2) \\ &\quad \times \exp(-4\sigma_p^2(\vec{k}_a + \vec{k}_b)^2) \end{aligned} \quad (6)$$

is the approximated biphoton wave function in the momentum basis. In these equations σ_p is the Gaussian width in the $\vec{x}_a + \vec{x}_b$ direction and controls the single-photon width: σ_c is the Gaussian width in the $\vec{x}_a - \vec{x}_b$ direction and controls the two photon correlation width. $N = (2\pi\sigma_p\sigma_c)^{-1}$ is a normalization constant.

To measure position correlations we put spatially resolving single-photon detectors at image planes of the SPDC source: to measure momentum correlations we put the detectors at Fourier transform planes of the source. For our purposes, then, random variable A corresponds either to the position or momentum of Alice's photon and B corresponds either to the position or momentum of Bob's photon.

The theoretical maximum mutual information for the wave function in Eq. (5) (measuring in the position basis)

$$I(A; B) = - \int p(\vec{x}_a, \vec{x}_b) \log\left(\frac{p(\vec{x}_a, \vec{x}_b)}{p(\vec{x}_a)p(\vec{x}_b)}\right) d\vec{x}_a d\vec{x}_b, \quad (7)$$

where $p(\vec{x}_a, \vec{x}_b) = |f(\vec{x}_a, \vec{x}_b)|^2$ and $p(\vec{x}_a) = \int |f(\vec{x}_a, \vec{x}_b)|^2 d\vec{x}_b$. For the momentum basis, the same relations hold, but the position variables are replaced by the momentum variables and the position wave function is replaced by the momentum wave function of Eq. (6).

For either basis, this theoretical maximum simplifies to

$$I(A; B) = \log\left(\frac{4\sigma_p^2 + \sigma_c^2}{4\sigma_c\sigma_p}\right)^2, \quad (8)$$

which is independent of detector characteristics. In the limit of strong correlations ($\sigma_p/\sigma_c \gg 1$), the mutual information reduces to $I(A; B) = \log(\sigma_p/\sigma_c)^2$. The ratio σ_p/σ_c is the familiar Fedorov ratio for quantifying entanglement—which is identical to the Schmidt number for Gaussian entangled states [21]. Our physical SPDC state had a beam envelope width of $\sigma_p = 1500 \mu\text{m}$ and a correlation width of approximately $\sigma_c = 40 \mu\text{m}$, resulting in an optimum mutual information from Eq. (8) of $I \cong 10$ bits/photon.

It should be noted that although we use pure quantum states, mutual information characterization can be applied to more general states including mixed states or bipartite multiparticle systems. For these situations, Eq. (7) would be valid but the probability distributions would be calculated in a different manner. Additionally, although we may be sacrificing some intuitive advantages by using an

entropic measure rather than dimensionality, we do gain a more direct link to information theory.

The measurement apparatus (shown in Fig. 1) consisted of a digital micromirror device (DMD) chip reflecting a portion of the signal or idler beam onto a single-photon counting module. The DMD chip allowed us to raster scan over the face of the beam in a controllable number of detection pixels, giving varying detector resolution. To incorporate the effects of the measurement apparatus, we integrate the probability density over the pixel area. For example, for position correlations between the m th pixel on Alice's detector, and the n th pixel on Bob's detector, the joint detection probability is

$$p(m, n) = \int_m d\vec{x}_a \int_n d\vec{x}_b |f(\vec{x}_a, \vec{x}_b)|^2. \quad (9)$$

The detected mutual information in either position or momentum is

$$I(A; B) = -\sum_m p(m) \log p(m) - \sum_n p(n) \log p(n) + \sum_{m,n} p(m, n) \log p(m, n), \quad (10)$$

where, for example,

$$p(m) = \sum_n p(m, n) \quad (11)$$

is the marginal probability for a pixel on Alice's detector.

With ideal alignment, a given pixel on Alice's detector will strongly correlate to only one pixel on Bob's detector. In practice, however, a relative lateral shift of pixels between Alice's and Bob's detectors—both vertically and horizontally—spreads correlations to four pixels at best. However, pixels far from the correlated pixel will still have no correlation. This was verified experimentally and it allowed us, for a given pixel on Alice's detector, to scan

only in a region of interest around the correlated pixel on Bob's detector, thus reducing the time required to complete a double raster scan.

Joint photon detection rates for the various raster scan measurements were between 1 and 100 per second (between correlated pixels). Integration time for raster scans was increased as the count rates decreased, with the longest time being 5 s per pixel pair. Multiple scans were performed for each detector resolution.

Both the predicted and experimentally measured values for mutual information are shown in Fig. 2. Mutual information values for both position correlation measurements and momentum correlation measurements are presented. For an accurate characterization, only the joint photon detection events are used to determine the mutual information. Single detection events without the corresponding detection in the other arm are ignored even for the calculation of the marginal probabilities of Eq. (11). Uncertainties in the number of detected photons N at each point in the double raster scan were assumed to be \sqrt{N} . This was used to find the uncertainties of the measured mutual information values, which agree with the statistics found by taking multiple data scans for a given detector resolution. It should be noted that this uncertainty calculation method does not take into account detector dark counts. Since the dark counts from each detector are uncorrelated, the dark coincident rate is much less than the coincident rate from the highly correlated SPDC state.

Light blue bars represent predicted mutual information values from numerical calculations of Eq. (10). The top of each bar corresponds to perfect lateral pixel alignment between Alice and Bob, and the bottom corresponds to relative lateral shifts, both horizontally and vertically, of half a pixel. These cases represent the maximum and minimum mutual information possible for a given number of detector pixels. The dark blue circles represent

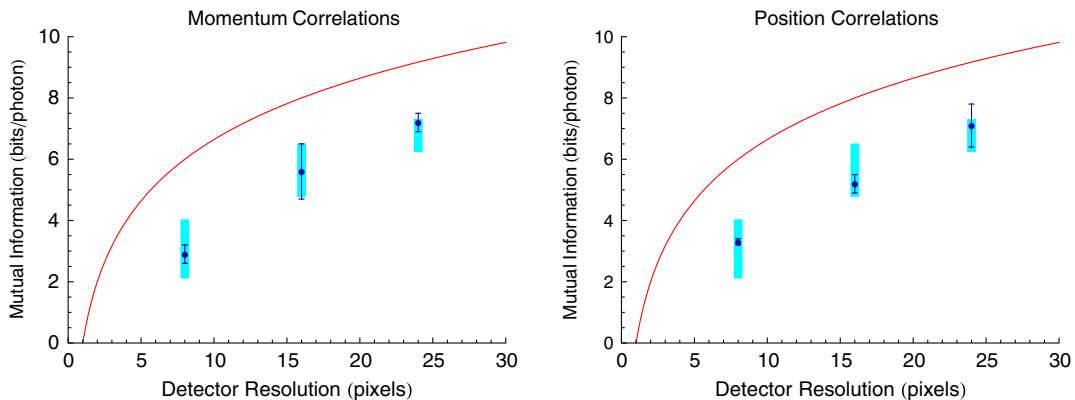


FIG. 2 (color online). Mutual information data for position correlation measurements and momentum correlation measurements are shown as a function of detector resolution. Data for detector resolutions of 8×8 pixels, 16×16 pixels, and 24×24 pixels are shown. The dark blue points with error bars are experimental data. The light blue bars are numerical simulations based on Eq. (10) both for the case of perfectly relative transversely aligned detectors and the case of a relative transverse misalignment of half a pixel. The red curve is the maximum mutual information that can be detected for the number pixels per detector.

experimentally measured channel capacities. The red curve gives the maximum mutual information that can be detected $I = \log(n \times n)$ for $n \times n$ pixels per detector (independent of state). The experimental data agree with the theoretically predicted values, staying within the predicted range for all data sets.

For momentum correlations a maximum mutual information of 7.2 ± 0.3 bits/photon was achieved; for position correlations only 7.1 ± 0.7 bits/photon were achieved. In principle, the two measurement bases should give the same mutual information. However, the alignment for position correlations was more sensitive—the reduction of mutual information for this basis most likely resulted from slight system misalignments.

The 576 dimensional measurement space is 16 times larger than the previous maximum for position-momentum entangled photons, and over 50 times larger than recent realizations using the photonic orbital angular momentum degree of freedom [17]. It should be noted that channel capacity characterization is different from using the channel for communication. When used for key distribution or communication, the characterized channel will indeed transmit 7 bits of information for a single joint detection event, despite the fact that characterization methods require many photon detection events. The use of this channel for key distribution or communication does, however, require some additional structure [11,12], and we are further investigating the ultimate experimental realization of these structures. It should be noted, however, that although we only detect photons from one pixel at a time, photons from the other pixels are not necessarily lost—rather, they are reflected to a different (but known) location that could in principle be monitored. This could be important in requirements for quantum information protocols, for example, in the detection of eavesdropping.

Recent work suggests that this data can be used to test for nonclassical behavior of the communication channel. A separable quantum state in two spatial dimensions satisfies the inequality $h(A|B)_P + h(A|B)_M \geq 2\log_2(\pi e)$, where, for example, $h(A)$ is the continuous (or differential) entropy of A , $h(A|B) = h(A, B) - h(B)$ is the conditional continuous entropy of A given B , and subscripts P or M indicate measurements in the position or momentum bases, respectively [19,22]. Although the inequality is derived using continuous entropies, Walborn *et al.* have made use of it with discrete entropies by approximating the relationship between the two entropies [23]. We make use of a modified inequality where the continuous entropy is replaced with the discrete entropy:

$$H(A|B)_P + H(A|B)_M \geq 2\log_2(\pi e) \approx 6.19. \quad (12)$$

It should be noted that we have not yet derived a proof of this form of the inequality and we are currently researching its full range of applicability.

From the 24×24 pixel scan data, we calculate

$$H(A|B)_P + H(A|B)_M = 2.2 \pm 0.7, \quad (13)$$

$$H(B|A)_P + H(B|A)_M = 2.2 \pm 0.6. \quad (14)$$

The separability bound of Eq. (12) is violated by more than 5 standard deviations, suggesting that the channel performance cannot be replicated classically.

In this Letter we have proposed and demonstrated a method of characterizing the quantum mutual information based channel capacity of a high-dimensional quantum communication channel using position and momentum entangled photons and a controllable pixel mirror. We measured up to 576 dimensions per detector, in both the position and the momentum basis, which resulted in a measured channel capacity of more than 7 bits/photon for either basis. The channel violated an entropic separability bound, strongly suggesting the performance cannot be replicated classically.

We acknowledge discussions with B.I. Erkmen and support from DARPA DSO InPho Grant No. W911NF-10-1-0404 and USARO MURI Grant No. W911NF-05-1-0197.

*Present address: Research Laboratory of Electronics, Massachusetts Institute of Technology, Cambridge, MA 02139, USA.

- [1] J.J. Sakurai, *Modern Quantum Mechanics* (Addison Wesley, Boston, 1993), revised ed.
- [2] M. A. Nielsen and I. L. Chuang, *Quantum Computation and Quantum Information* (Cambridge University Press, Cambridge, U.K., 2004).
- [3] J. T. Barreiro, N. K. Langford, N. A. Peters, and P. G. Kwiat, *Phys. Rev. Lett.* **95**, 260501 (2005).
- [4] A. V. Sergienko and G. S. Jaeger, *Contemp. Phys.* **44**, 341 (2003).
- [5] G. Molina-Terriza, J. P. Torres, and L. Torner, *Nature Phys.* **3**, 305 (2007).
- [6] L. Chen, J. Leach, B. Jack, M. J. Padgett, S. Franke-Arnold, and W. She, *Phys. Rev. A* **82**, 033822 (2010).
- [7] I. Ali-Khan, C. J. Broadbent, and J. C. Howell, *Phys. Rev. Lett.* **98**, 060503 (2007).
- [8] S. P. Walborn, D. S. Lemelle, D. S. Tasca, and P. H. Souto Ribeiro, *Phys. Rev. A* **77**, 062323 (2008).
- [9] M. N. O'Sullivan-Hale, I. Ali Khan, R. W. Boyd, and J. C. Howell, *Phys. Rev. Lett.* **94**, 220501 (2005).
- [10] S. P. Walborn, D. S. Lemelle, M. P. Almeida, and P. H. Souto Ribeiro, *Phys. Rev. Lett.* **96**, 090501 (2006).
- [11] A. K. Ekert, *Phys. Rev. Lett.* **67**, 661 (1991).
- [12] C. H. Bennett and S. J. Wiesner, *Phys. Rev. Lett.* **69**, 2881 (1992).
- [13] J.-L. Chen, C. Wu, L. C. Kwek, C. H. Oh, and M.-L. Ge, *Phys. Rev. A* **74**, 032106 (2006).
- [14] L. Zhang, C. Silberhorn, and I. A. Walmsley, *Phys. Rev. Lett.* **100**, 110504 (2008).

- [15] J.B. Pors, A. Aiello, S.S.R. Oemrawsingh, M.P. van Exter, E.R. Eliel, and J.P. Woerdman, *Phys. Rev. A* **77**, 033845 (2008).
- [16] J.B. Pors, S.S.R. Oemrawsingh, A. Aiello, M.P. van Exter, E.R. Eliel, G.W. 't Hooft, and J.P. Woerdman, *Phys. Rev. Lett.* **101**, 120502 (2008).
- [17] A.C. Dada, J. Leach, G.S. Buller, M.J. Padgett, and E. Andersson, *Nature Phys.* **7**, 677 (2011).
- [18] C.E. Shannon and W. Weaver, *The Mathematical Theory of Communication* (University of Illinois Press, Champaign, 1998).
- [19] T. Cover and J. Thomas, *Elements of Information Theory* (Wiley, New York, 1991).
- [20] C.K. Law and J.H. Eberly, *Phys. Rev. Lett.* **92**, 127903 (2004).
- [21] M.V. Fedorov, Y.M. Mikhailova, and P.A. Volkov, *J. Phys. B* **42**, 175503 (2009).
- [22] I. Bialynicki-Birula and J. Mycielski, *Commun. Math. Phys.* **44**, 129 (1975).
- [23] S.P. Walborn, A. Salles, R.M. Gomes, F. Toscano, and P.H. Souto Ribeiro, *Phys. Rev. Lett.* **106**, 130402 (2011).